# High efficiencies in the electrochemical oxidation of an anthraquinonic dye with conductive-diamond anodes

José Mario Aquino[1], Romeu C. Rocha-Filho[1], Cristina Sáez[2], Pablo Cañizares[2,] Manuel A. Rodrigo[2,*]

(1) Departmento de Química, Universidade Federal de São Carlos, C. P. 676, 13560-970 São Carlos - SP, Brazil
(2) Department of Chemical Engineering, Facultad de Ciencias y Tecnologías Químicas, Universidad de Castilla La Mancha, Campus Universitario s/n, 13071 Ciudad Real, Spain

*Corresponding author. Tel.: +34 926902204100x3411; fax: +34 926295318

E-mail address: manuel.rodrigo@uclm.es (M.A. Rodrigo)

**Abstract**

Oxidation of anthraquinonic dye Acid Blue 62 by electrolysis with conductive-diamond electrodes is studied in this work. COD, TOC and color have been selected to monitor the degradation of the molecule as a function of several operating inputs (current density, pH, temperature, and NaCl concentration). Results show that the electrochemical oxidation of this model of large molecules follows a first order kinetics in all the conditions assessed, and it does not depend on the pH and temperature. The occurrence of chloride ions in wastewaters increases the rate of color and COD removal as a consequence of the mediated oxidation promoted by the chlorinated oxidizing species. However, chloride occurrence does not have an influence on the mineralization rate. First-order kinetic-constants for color depletion (attack to chromophores groups), oxidation (COD removal) and mineralization (TOC removal) were found to depend on the current density and to increase significantly with its value. A single model was proposed to explain these changes in terms of the mediated oxidation processes. Rate of mineralization remained very close to that expected for a purely mass-transfer controlled process. This was explained assuming that mediated oxidation does not have a significant influence on the mineralization in spite it has some effect on intermediate oxidation stages. The efficiency of the oxidation was found to depend mainly on the concentration of COD being negligible the effect of the other inputs assessed except for the occurrence of chloride ions. Opposite, the efficiency of mineralization depends on concentration of TOC and current density and it did not depend on the chloride occurrence. This observation was found to have an important influence on the power required to remove a given percentage of the initial TOC or COD. To decrease COD efficiently it is very important the occurrence of chloride in the solution, while to remove TOC efficiently it is more important to work at low current densities and chloride effect is negligible. Energy consumption could be decreased by folds using the proper conditions.

**Keywords:** Electrochemical degradation**,** mineralization, chloride-mediated oxidation, mass-transfer controlled reactions, kinetic modeling, boron-doped diamond electrode.

## 1. Introduction

Boron-doped diamond (BDD) has been extensively used as an anode material to promote the electrochemical oxidation of a series of organic pollutants, due to its ability to produce quasi-free hydroxyl radicals (•OH) [1]. As the concentration of these radicals exponentially decays from the BDD surface into the Nernst diffusion layer, the oxidation depends on the mass transport of organics from the bulk to a region close to the anode surface, if the reaction between •OH radicals and the organic pollutants is fast. Thus, a kinetic model was developed by Comninellis' group [2-6] relating a commonly measured parameter, such as the chemical oxygen demand (*COD*), to the processes that occur close to the anode (reaction cage), independently of the nature of the organic pollutant. The adjustable parameters of that model, which also dictate the efficiency of the electrochemical oxidation, are the current density and the mass-transfer coefficient (that depends on the hydrodynamic conditions). Besides the reaction with organic compounds, the quasi-free •OH radicals may oxidize inorganic ions to yield strong oxidants[7], such as persulfate, percarbonate, perphosphate or the chloro oxidant species ($Cl_2$, HOCl and $OCl^-$, or undesired $ClO_3^-$ and $ClO_4^-$) that can indirectly oxidize organic pollutants (mediated oxidation), as previously shown by Panizza *et al.* [2]. The contribution of mediated oxidation was taken into account by Cañizares *et al*. [8-9]through a simplified kinetic model, in which the electrochemical reactor was divided into three stirred tank reactors corresponding to the electrochemical zones (one close to the anode and the other to the cathode) and the chemical zone. Subsequently, in another work, Cañizares' group [10] took into account the effect of the chemical reaction to successfully model the electrochemical oxidation of phenolic wastes on a BDD anode.

To model a mass transport-controlled wastewater treatment process, two kinetic expressions should be used: one to define the mass-transport process and another for the mediated oxidation. The kinetics of mass transfer and the electron transfer rate can be defined by equation 1. Under mass transport controlled reaction conditions, the concentration of the pollutant on the electrode surface ($[C]_s$) should be negligible because every molecule that reaches the electrode surface is immediately oxidized. Then, eq. 1 can be simplified to eq. 2, which is typical of a first-order kinetic process.

$$r_{\text{m.t.}} = k_{\text{L}} \cdot A \cdot \left([C]_{\text{b}} - [C]_{\text{s}}\right) \qquad (1)$$

$$r_{\text{d.e.p.}} = \frac{I_{\text{L}}}{\text{n} \cdot F} = k_{\text{L}} \cdot A \cdot [C]_{\text{b}} \qquad (2)$$

where $r_{\text{m.t.}}$ and $r_{\text{d.e.p.}}$ are the mass transfer rate and direct electrochemical process rate (mol $s^{-1}$), respectively, $k_{\text{L}}$ is the mass-transfer coefficient (m $s^{-1}$), $A$ the electrode area ($m^2$), $[C]_{\text{b}}$ the

concentration of the pollutant in the solution bulk (mol $m^{-3}$), $I_L$ is the electrical current (A), $n$ the number of transferred electrons, and $F$ the Faraday constant (96485 C $mol^{-1}$).

Mediated electrooxidation processes (med.e.p.) can be modeled by a second-order kinetic equation, according to eq. 3:

$$r_{\text{med.e.p.}} = k_{\text{ox}} \cdot [Ox] \cdot [C]_{\text{b}} \qquad (3)$$

where $r_{\text{med.e.p.}}$ is the rate of the mediated electrooxidation process (mol $s^{-1}$), $k_{\text{ox}}$ its rate constant ($mol^{-1}$ $m^6$ $s^{-1}$), and [$Ox$] the concentration of oxidants produced during the electrolytic process (mol $m^{-3}$).

This second-order kinetic equation can also be simplified to a first-order kinetic equation assuming that oxidants produced and consumed during the electrochemical processes reach a constant pseudo-steady-state (pss) concentration in every electrolysis:

$$r_{\text{med.e.p}} = k_{\text{med}} \cdot [C]_{\text{b}} \qquad (4)$$

where a new kinetic constant $k_{\text{med}}$ is defined as

$$k_{\text{med}} = k_{\text{ox}} \cdot [Ox]_{\text{pss}} \qquad (5)$$

A mass balance of this discontinuous process leads to eq. 6,which is a model of the process dynamics.

$$V \frac{\text{d}[C]_{\text{b}}}{\text{d}t} = k_{\text{L}} \cdot A \cdot [C]_{\text{b}} + k_{\text{med}} \cdot [C]_{\text{b}} \qquad (6)$$

where $V$ is the electrolyzed solution volume ($m^3$).

Integration of eq. 6 results in eq. 7, in which it can be observed that both kinetic constants are contained in the slope ($k_{\text{exp}}$) of the semi-logarithmic linear plot (ln [$C_b$] *vs.* $t$); once the value of $k_L$ is determined, that of $k_{\text{med}}$ can be easily determined.

$$\ln\left(\frac{[C]_{\text{b}}}{[C]_{\text{b0}}}\right) = \left(\frac{k_{\text{L}} \cdot A + k_{\text{med}} \cdot V}{V}\right) \cdot t = k_{\text{exp}} \cdot t \qquad (7)$$

This model can be used with total organic carbon (*TOC*), *COD* or with the raw pollutant concentration ($[C]_b$). However, it will have different values for each parameter because, despite

the mass transfer contribution being the same for every parameter, the mediated oxidation kinetics is not the same for oxidizing functional groups (color) or mineralizing the molecule (*TOC*).

Moreover, recently many works have been focused on the removal of dyes looking for possible industrial applications; however this manuscript is focused on the kinetic mechanisms of the oxidation of large molecules using a BDD anode. As a consequence of steric effects, dyes can be used as models of molecules whose size is large enough to hinder their direct oxidation on an electrode surface. On the other hand, chromophore groups are easily oxidized by chemical oxidants in the bulk. This means that mediated oxidation processes are expected to have a significant role in the overall oxidation process. Consequently, the typical control of the oxidation rate by diffusion-controlled processes should be explained in terms of the hard oxidation conditions near the electrode surface (reaction cage) and not of direct electrochemical oxidation processes.

Thus, the electrochemical degradation of an anthraquinonic dye (Acid Blue 62 – AB 62) will be investigated with respect to some operational inputs (current density, pH, NaCl concentration, and temperature). Then, the analytical parameters (*COD, TOC,* and absorbance) commonly used to follow the removal of this pollutant will be compared to the ones of a kinetic model theoretically developed for oxidation on a BDD anode using simple molecules, under mass transport control.

## 2. Materials and methods

### *2.1 Chemicals*

All chemicals, including NaCl (a.r.,Panreac), $Na_2SO_4$ (a.r., Panreac), $H_2SO_4$ (a.r. Sigma-Aldrich), NaOH (a.r. Panreac), and Acid Blue62 (Quimanil, industrial grade), were used as received. The dye content in the Acid Blue 62 sample was estimated as about 70% using *TOC* measurements. Doubly deionized water (Millipore Milli-Q system, resistivity $\geq$ 18.2 MΩ cm) was used for the preparation of all solutions.

### *2.2 Electrochemical degradation experiments*

The electrochemical experiments were carried out in a single-compartment filter-press flow cell operating in batch mode. Boron-doped diamond (BDD) and stainless steel (AISI 304) circular plates were used as anode and cathode, respectively. The BDD anode was assembled on a circular stainless steel plate using a silver paste for electric contact. The geometric area and inter-electrode distance were 78 $cm^2$ and 9 mm, respectively. The BDD film (Adamant Technologies, Switzerland) was deposited on a monocrystalline p-doped silicon substrate by the

hot filament chemical vapor deposition (HFCVD) technique, with specified boron content of 500 ppm.

The investigated variables and their values were current density (10, 30, and 50 mA $cm^{-2}$), pH (3, 7, and 11), NaCl concentration (0, 20, and 40 mmol $dm^{-3}$), and temperature (15, 35, and 55 ºC). All the experiments were carried out using 0.6 $dm^3$ of a 100 mg $dm^{-3}$ (0.25 mmol $dm^{-3}$) aqueous solution of AB 62 in 0.1 mol $dm^{-3}$ $Na_2SO_4$, at a flow rate of 400 $dm^3$ $h^{-1}$. The solution pH was continuously monitored and fixed at the desired value by additions of concentrated or diluted solutions of $H_2SO_4$ or NaOH.

*2.3 Analyses*

The specific attack to the chromophore was followed through the color abatement of the dye solution; thus, UV-vis spectra were obtained at certain time intervals from 200 nm to 800 nm using an UV-1603 spectrophotometer from Shimadzu, until complete decolorization was attained. The *COD* value (determined by the colorimetric method), which indicates the progress of the organics oxidation, was continuously monitored until its complete removal by sampling 2 $cm^3$ of the electrolyzed solution at certain time intervals. The *TOC* value (determined by the high-temperature combustion method),which provides information about the conversion of organic pollutants to $CO_2$, was similarly monitored (5 $cm^3$samples). The complete analytical procedures used in the *COD* and *TOC* determinations are described elsewhere [11].

The instantaneous current efficiency (*ICE*) for the electrochemical degradation of the AB 62 dye was calculated for the *COD* and *TOC* variations, according to:

$$ICE_{COD} = \frac{[(COD)_t - (COD)_{t+\Delta t}]\cdot F\cdot V}{8\cdot I\cdot \Delta t} \qquad (8)$$

$$ICE_{TOC} = \frac{2.67\cdot [(TOC)_t - (TOC)_{t+\Delta t}]\cdot F\cdot V}{8\cdot I\cdot \Delta t} \qquad (9)$$

where $COD_t$ and $COD_{t+\Delta t}$ or $TOC_t$ and $TOC_{t+\Delta t}$ are the *COD* or *TOC* values (g $dm^{-3}$) at times $t$ and $t+\Delta t$, respectively, 2.67 is the conversion factor between *COD* and *TOC*, as described by Gray and Becker [12], $F$ the Faraday constant (96485 C $mol^{-1}$), and $I$ the applied electrical current (A).

The electric energy consumption per unit volume of electrolyzed solution ($w$) was calculated using the following equation:

$$w = \frac{U\cdot I\cdot t}{V} \qquad (10)$$

where $U$ is the cell voltage (V).

## 3. Results and discussion

Figures 1 and 2 show the changes in the *COD*, *TOC* and color as a function of the applied electrical charge per unit volume of electrolyzed solution ($Q_{ap}$), during several electrolyses of a 0.25 mmol $dm^{-3}$ AB 62 solution, carried out at different current densities and with different compositions in terms of chloride ions. Before discussing the figures, it is worthwhile to clarify that each of these characterization parameters accounts for a different oxidation concept and that unfortunately they are frequently confused in the literature, suggesting that they are equivalent. Color is directly related to the concentration of the dye and its removal means an initial oxidation stage in the mineralization of the molecule in which a chromophore group is attacked (it is simply a transformation of the dye molecule into intermediates). Consequently, color is the parameter that changes faster during the first stage of the electrolysis, being rapidly depleted. On the contrary, *TOC* indicates the complete mineralization of the dye molecule, *i.e.* the transformation of the organic carbon into carbon dioxide, a process that in the case of a large molecule will occur via the formation of intermediates due to the large number of electrons that need to be transferred. From *TOC* it is not possible to differentiate between the raw dye and its intermediates (it does not inform about the progress of the oxidation) and its change only quantifies the fraction of the dye molecules that has been completely mineralized. This explains why it behaves as the slowest parameter to be depleted and should be considered as the main pollution indicator in the treatment of a dye. *COD* is an in-between parameter, which indicates the progress of the oxidation process not only based on the direct attack to a particular group or on the total oxidation of the molecule, but actually accounting for every oxidation undergone by the dye molecule or its oxidation intermediates. At the final stages of the electrolysis of a dye, commonly *COD* has a very small value while *TOC* is still significant, because of the large oxidation state of the intermediates formed. This means that although the three parameters account for the pollution of a wastewater, color or *TOC* are good parameters to follow the initial stage in the treatment of a large molecule or to assess the total depletion caused by the treatment, respectively, whereas *COD* is the best parameter to follow the course of the degradation itself.

Taking this into account, the oxidation of large molecules with conductive-diamond electrolyses follows first-order kinetics (linear trend in the semi-logarithmic plot) in all the conditions assessed and with the three parameters monitored, as can be observed in Figs. 1 and 2. For *COD* and absorbance, there is a huge difference between results obtained in the treatment of the AB62 dye in the absence or presence of chloride ions, the process being more efficient in the latter case. This is a surprising result because the production of powerful oxidation species during the electrolysis of organics with conductive-diamond anodes is known to be attained with both

chloride (active chlorine, chlorate and perchlorate) and sulfate media (peroxodisulfate); indeed larger efficiencies for electrolyses in sulfate media compared to the chloride media were reported in several papers [13-17]. Those results had been explained in terms of the slow oxidation kinetics of organics by chlorate and perchlorate at room temperature [13]. The larger efficiencies observed in this work clearly indicate that the formation of these oxoanions should not be promoted in the presence of sulfate and that these negative effects are not very important. The effect of the presence of NaCl in the electrochemical oxidation of different organics has been reported in the literature, and it seems to also depend on the nature of the organics, concentration, pH, and applied current density. For instance, Scialdone *et al*. [18] compared the electrochemical oxidation of oxalic acid (OA) at BDD and DSA® anodes in the presence and absence of NaCl. As it is known, the use of DSA® electrodes promotes the formation of large amounts of active chlorine that seems to successfully attack the OA molecule. This can explain the higher removal percentages obtained in the presence of NaCl. Wu *et al*. [19] also observed an increase in the *COD* removal during the electrolysis of 1000 mg $dm^{-3}$ of the Methylene Blue dye in a conventional electrochemical cell using both BDD and DSA® anodes in the presence of NaCl. On the other hand, Cabeza *et al*. [20] did not observe significant differences between the experimental and theoretical (based on a mass transfer model) values of *COD* removal during the electrochemical degradation of a landfill leachate effluent in the presence of NaCl. Aquino *et al*. [16] even observed a superior *COD* removal in the absence of NaCl during the electrochemical treatment of a real textile effluent using a BDD anode. The expected lower efficiency of the BDD anode towards organic pollutant removal in the presence of chloride ions can be occasioned by a low availability of •OH radicals [21-22], due to their reaction with chloride ions to produce $ClO_3^-$or $ClO_4^-$ [23] and even form chloro radicals [24].

Once the role of NaCl is clarified, although an influence of the current density on the *COD* removals values is observed, the results are far from those expected. Thus, in every case (sulfate and chloride) the efficiencies are much greater than expected according to a simple mass-transfer electrolytic model (plotted in Fig. 1). Naturally, this model indicates that the process should be more efficient working under low current densities (and also high flow rates); however, the results account for the importance of mediated electrochemical processes in the removal of large molecules and not for direct electrochemical processes. At this point, it is worthwhile to point out that the initial concentration of the AB 62 dye (100 mg $dm^{-3}$ COD) is below the mass-transfer limit concentration for the used current densities in this type of cell. Thus a standard mass-transport characterization test with the $Fe(CN)_6^{3-}/Fe(CN)_6^{4-}$ redox couple [25] gives a $k_L$ value of the electrochemical cell within the fluid dynamic conditions used (400 $dm^3$ $h^{-1}$, 298 K) of $1.28 \times 10^{-5}$ m $s^{-1}$ [26]. The value of the limiting current density for the initial concentration (this value decreases linearly with the concentration) is about 1.5 mA $cm^{-2}$, which is significantly below the range of current densities applied in this work (10-50 mA $cm^{-2}$).

Changes in the *TOC* and color removals also follow a first-order kinetics, with a linear trend in the semi-logarithmic plot (just some points at the end of the electrolyses differ from this trend), as can be seen in Fig. 2b. In the case of color removal, the marked difference between the results obtained in the presence or absence of chloride ions is also noticed, but in the case of *TOC* removal these differences are smaller and the current density starts to play a more significant role. In addition, as expected for a direct electrochemical oxidation process, the most efficient mineralization conditions are those in which the current density values were low. This confirms that although the contribution of mediated oxidation is very important, direct electrolysis (or at least processes occurring close to the anode surface) is essential for mineralization. As expected, the removal of color (transformation of the initial dye molecule into an intermediate) is significantly faster, since the chloro oxidant species (HOCl and $OCl^-$) can easily attack electron rich groups of the dye molecule through addition, substitution or oxidation reactions [27]. This promotes the rapid formation of intermediates than can be further oxidized as the process proceeds.

Figure 3 shows the influence of current density and NaCl concentration on the fitting first-order kinetic constants for color, *COD* and *TOC* removal. These kinetic constants were calculated from the slope of semi-logarithmic *vs.* time plots. For the case of *COD* and *TOC,* the complete set of data was used to fit the constant, whereas for the case of color only the points corresponding to the first oxidation stage (which fit well to this trend) were used. In this latter case, a change in the slope is commonly found for large values of $Q_{ap}$, as apparent in Fig. 2, due to competing oxidation reactions of the dye and other intermediate compounds, when differences in oxidizability might become important. These kinetic constants should be interpreted in terms of the following equation, obtained by combining equations 5 and 7:

$$\ln\left(\frac{[C]_b}{[C]_{b0}}\right) = \left[\frac{k_L \cdot A + \left(k_{ox}[Ox]_{pss}\right)\cdot V}{V}\right] \cdot t \qquad (11)$$

As can be observed in Fig. 3a, very different values of the kinetic constants were obtained for the color, *COD*, and *TOC* removals; however, in every case a slight increase is observed with the current density. Taking into account eq. 11, this trend can be easily explained in terms of promotion of the formation of higher concentrations of intermediates as the current density increases, because the mass-transfer coefficient, the electrode surface, and the reaction volume do not change. To understand these differences, the different meanings of the three parameters (*COD*, *TOC*, and color) have to be taken into account. The slope of the linear trend is similar for *COD* and *TOC*, suggesting that mineralization might be considered as the main oxidation process. On the contrary, the color removal does not seem to be strongly influenced by the current density, possibly because of the great value of $k_{ox}$ for this process, which helps to rapidly deplete the color during the treatment, or because of the equivalent effect on the depletion of color brought on by

the larger number and the higher concentration of oxidants (quantified as [*Ox*]) that can attack the chromophore groups.

The expected kinetic constant for a purely mass transport-controlled process is also plotted in Fig. 3. As can be observed, the values of the kinetic constants are mostly greater than the expected values for a purely mass transport-controlled process. Differences are greater for color removal and smaller for *TOC* removal, suggesting that (according to eq. 11) $k_{med}$ ($k_{ox}[Ox]_{pss}$) is very significant for the initial oxidation, but not much for the mineralization process. This means that mediated oxidants play an important role in the oxidation of chromophore groups and a lesser, but still important, role in the mineralization process.

Figure 3b shows the effect of NaCl concentration on the kinetic constants. As discussed above, the influence of mediated oxidation is higher for color and *COD* removal, whose kinetics is significantly improved in the presence of small concentrations of NaCl. The kinetic constant for color removal in the absence of NaCl is slightly higher than those for *COD* and *TOC* removal. This fact could be related to the role of peroxodisulfate ions in the mediated oxidation [28]. On the other hand, mineralization does not seem to be significantly influenced by the NaCl concentration, as the electrogenerated chloro oxidant species are incapable of converting the intermediate compounds to $CO_2$. Thus, the kinetic constant for *TOC* removal remained close to the one theoretically calculated for a direct process under mass-transfer control. The possible loss of *TOC* removal efficiency in the presence of chloride ions, due to the generation of organochlorine byproducts was not observed.

Figure 4 shows the effect of temperature and pH on the kinetic constants of the electrochemical oxidation process. Initially, it could be expected that mediated oxidation carried out by the chlorinated oxoanions or by peroxodisulfate ions should be influenced by both parameters; similarly, a higher mineralization rate with temperature and at acidic pH could also be expected because of the greater effects of both oxidants at these conditions. However, the small influence observed (almost null and negligible in every case), in particular if the effect is compared to that of the current density, indicates that this is not the case and that both parameters have no significant influence on the oxidation rate. Similar results have been reported in the literature [27-29] for the removal of different organics. Pereira *et al*. [29], who reported on the electrochemical degradation of bisphenol A in a flow reactor with a BDD anode, also observed that pH does not influence markedly the *COD* removal, which is slightly improved by changes in the temperature from 25 to 40 ºC. On the contrary, Panizza *et al*. [28] observed that an increase in temperature promotes the decomposition of peroxodisulfate ions, thus negatively affecting the BDD-electrochemical oxidation of the Acid Blue 22 dye. In addition, Bensalah *et al*. [30] also observed a negligible increase in the oxidation rate of the Alphazurine A dye, when its electrooxidation was carried out in the range of 25 to 60 °C.

Figure 5 shows the effect of the concentration of organics (*TOC* or *COD*), temperature or sodium chloride concentration, and current density on the instantaneous current efficiency (*ICE*). As can be observed, concentration is the most relevant parameter: the *ICE* values diminish as the concentration decreases. This effect is especially important for very small concentrations (in which a small decrease of 10% leads to more than one order of magnitude drop in the efficiency) and less significant but still appreciable at higher concentrations of organics (logarithmic scale). On the other hand, the effect of the current density, temperature or sodium chloride concentration is less significant and a cloud of points is observed without a clear trend. Just the points corresponding to a nil content of chloride show a significantly less efficient behavior for the oxidation (*COD*), although there is no significant influence on the efficiency of mineralization (*TOC*), indicating that chlorine, as explained before, has a significant role in the oxidation of the dye to intermediates but has no influence on its conversion to carbon dioxide, which does not depend on the concentration of chloride in the supporting media. The expected *ICE* behaviors according to a mass transport model for the three applied current densities are also depicted in Fig. 5. As can be observed, an effect of current density on *ICE* is expected for a purely mass transfer-controlled process, contrary to obtained results. In addition, most *ICE* values are greater than the ones expected for a purely mass transport-controlled process in terms of *COD* (even for the condition in the absence of NaCl), but not in terms of *TOC* in which points lay over the lines proposed by the mass transfer model. This means that many of the oxidation processes are occurring in the bulk but the mineralization is attained near the electrode surface by direct oxidation or by the action of strong oxidants such as hydroxyl radicals.

These changes in the efficiency have an important influence on the power required to remove a percentage of the initial *TOC* or *COD*, although it is also important to take into account the cell voltage. Figure 6 shows the variation of energy consumption (*w*) with the percentage removal of *COD* and *TOC*. In chloride media energy consumptions as low as 10 kW h $m^{-3}$ are required to attain the complete COD removal, independently of the operating conditions. However, in the absence of NaCl this value increases abruptly (around ten times). On the other hand, energy consumptions around 100 kW h $m^{-3}$ are required for complete mineralization of the organics both in the presence or absence of chloride ions. The difference between both values should be explained in terms of the accumulation of carboxylic acids at the latter stages of the electrolytic process because these species have an almost nil theoretical *COD* and still a significant *TOC* value. As observed, cost can significantly decrease if the right conditions are used. Finally, it should be noted that to efficiently remove *COD* the presence of chloride ions is very important to promote mediated oxidation processes, whereas to efficiently remove *TOC* the use of low current densities is very important to promote oxidation near the anode surface.

**Conclusions**

From this work, the following conclusions can be drawn:

1. The electrochemical degradation of the Acid Blue 62 dye was successfully attained using a BDD anode in the presence and absence of chloride ions. Chloride ions present in solution lead to increased rates of color and *COD* removal as a consequence of the mediated oxidation promoted by the chlorinated oxidizing species. However, this has no influence on the mineralization rate.
2. Contrary to what it could be expected for a process in which mediated oxidation plays a significant role, a very small influence of pH and temperature on the reaction rate and efficiencies was observed during the oxidation of AB62.
3. The obtained first-order kinetic constants for color removal (attack on the chromophores groups), oxidation (*COD* removal), and mineralization (*TOC* removal) depend on the current density and increase significantly with its value.
4. The obtained first-order kinetic constants for mineralization remained very close to that of a purely mass transfer-controlled process, indicating that most mineralization processes should occur not in the bulk but near the electrode surface, in accordance with the reaction cage model proposed by the group of Comninellis.
5. The efficiencies for color and COD removal depend mainly on the organics concentration and the presence of chloride ions in solution. For the mineralization process, these efficiencies do not depend on the presence of chloride ions, but they depend significantly on the current density; thus, the process is more efficient when carried at low current densities. The energy consumption can be significantly decreased if adequate conditions are chosen.

**Acknowledgements**

This work was supported by the MCT (Ministerio de Ciencia y Tecnología, Spain) through the project CTM2010-18833/TECNO. The Brazilian funding agencies CNPq and CAPES (for the scholarship awarded to J.M. Aquino) and the company Quimanil (for supplying the dye samples) are also acknowledged.

**References**

[1] Kapałka, A.; Fóti, G.; Comninellis, C. The importance of electrode material in environmental electrochemistry. Formation and reactivity of free hydroxyl radicals on boron-doped diamond electrodes. *Electrochim. Acta*, **2009**, *54*, 2018-2023.

[2] Panizza, M.; Michaud, P.A.; Cerisola, G.; Comninellis, C. Anodic oxidation of 2-naphthol at boron-doped diamond electrodes. *J. Electroanal. Chem.*, **2001**, *507*, 206-214.

[3] Comninellis, C. Electrocatalysis in the electrochemical conversion/combustion of organic pollutants for waste water treatment. *Electrochim. Acta*, **1994**, *39*, 1857-1862.

[4] Panizza, M.; Michaud, P.A.; Cerisola, G.; Comninellis, C. Electrochemical treatment of wastewaters containing organic pollutants on boron-doped diamond electrodes: Prediction of specific energy consumption and required electrode area. *Electrochem. Commun.*, **2001**, *3*, 336-339.

[5] Simond, O.; Schaller, V.; Comninellis, C. Theoretical model for the anodic oxidation of organics on metal oxide electrodes. *Electrochim. Acta*, **1997**, *42*, 2009-2012.

[6] Kapałka, A.; Fóti, G.; Comninellis, C. Kinetic modelling of the electrochemical mineralization of organic pollutants for wastewater treatment. *J. Appl. Electrochem.*, **2008**, *38*, 7-16.

[7] Panizza, M.; Cerisola, G. Direct and mediated anodic oxidation of organic pollutants. *Chem. Rev.*, **2009**, *109*, 6541-6569.

[8] Cañizares, P.; García-Gómez, J.; Lobato, J.; Rodrigo, M.A. Modeling of wastewater electro-oxidation processes part II. Application to active electrodes. *Ind. Eng. Chem. Res.*, **2004**, *43*, 1923-1931.

[9] Cañizares, P.; García-Gómez, J.; Lobato, J.; Rodrigo, M.A. Modeling of wastewater electro-oxidation processes part I. General description and application to inactive electrodes. *Ind. Eng. Chem. Res.*, **2004**, *43*, 1915-1922.

[10] Cañizares, P.; Lobato, J.; Paz, R.; Rodrigo, M.A.; Sáez, C. Electrochemical oxidation of phenolic wastes with boron-doped diamond anodes. *Water Res.*, **2005**, *39*, 2687-2703.

[11] Aquino, J.M.; Rocha-Filho, R.C.; Rodrigo, M.A.; Sáez, C.; Cañizares, P. Electrochemical degradation of the Reactive Red 141 dye using a boron-doped diamond anode. *Water Air Soil Pollut.*, **2013**, *224*, 1397.

[12] Gray, S.R.; Becker, N.S.C. Contaminant flows in urban residential water systems. *Urban Water*, **2002**, *4*, 331-346.

[13] Cañizares, P.; Martínez, L.; Paz, R.; Sáez, C.; Lobato, J.; Rodrigo, M.A. Treatment of Fenton-refractory olive oil mill wastes by electrochemical oxidation with boron-doped diamond anodes. *J. Chem. Technol. Biotechnol.*, **2006**, *81*, 1331-1337.

[14] Murugananthan, M.; Yoshihara, S.; Rakuma, T.; Shirakashi, T. Mineralization of bisphenol A (BPA) by anodic oxidation with boron-doped diamond (BDD) electrode. *J. Hazard. Mater.*, **2008**, *154*, 213-220.

[15] Murugananthan, M.; Latha, S.S.; Raju, G.B.; Yoshihara, S. Anodic oxidation of ketoprofen - An anti-inflammatory drug using boron doped diamond and platinum electrodes. *J. Hazard. Mater.*, **2010**, *180*, 753-758.

[16] Aquino, J.M.; Pereira, G.F.; Rocha-Filho, R.C.; Bocchi, N.; Biaggio, S.R. Electrochemical degradation of a real textile effluent using boron-doped diamond or β-$PbO_2$ as anode. *J. Hazard. Mater.*, **2011**, *192*, 1275-1282.

[17] Solano, A.M.S.; de Araújo, C.K.C.; de Melo, J.V.; Peralta-Hernandez, J.M.; da Silva, D.R.; Martínez-Huitle, C.A. Decontamination of real textile industrial effluent by strong oxidant species electrogenerated on diamond electrode: Viability and disadvantages of this electrochemical technology. *Appl. Catal., B*, **2013**, *130-131*, 112-120.

[18] Scialdone, O.; Randazzo, S.; Galia, A.; Silvestri, G. Electrochemical oxidation of organics in water: Role of operative parameters in the absence and in the presence of NaCl. *Water Res.*, **2009**, *43*, 2260-2272.

[19] Wu, M.; Zhao, G.; Li, M.; Liu, L.; Li, D. Applicability of boron-doped diamond electrode to the degradation of chloride-mediated and chloride-free wastewaters. *J. Hazard. Mater.*, **2009**, *163*, 26-31.

[20] Cabeza, A.; Urtiaga, A.M.; Ortiz, I. Electrochemical treatment of landfill leachates using a boron-doped diamond anode. *Ind. Eng. Chem. Res.*, **2007**, *46*, 1439-1446.

[21] Polcaro, A.M.; Vacca, A.; Mascia, M.; Palmas, S.; Ruiz, J.R. Electrochemical treatment of waters with BDD anodes: kinetics of the reactions involving chlorides. *J. Appl. Electrochem.*, **2009**, *39*, 2083-2092.

[22] Mascia, M.; Vacca, A.; Polcaro, A.M.; Palmas, S.; Ruiz, J.R.; Pozzo, A.D. Electrochemical treatment of phenolic waters in presence of chloride with boron-doped diamond (BDD) anodes: Experimental study and mathematical model. *J. Hazard. Mater.*, **2010**, *174*, 314-322.

[23] Sánchez-Carretero, A.; Sáez, C.; Cañizares, P.; Rodrigo, M.A. Electrochemical production of perchlorates using conductive diamond electrolyses. *Chem. Eng. J.*, **2011**, *166*, 710-714.

[24] Grebel, J.E.; Pignatello, J.J.; Mitch, W.A. Effect of halide ions and carbonates on organic contaminant degradation by hydroxyl radical-based advanced oxidation processes in saline waters. *Environ. Sci. Technol.*, **2010**, *44*, 6822-6828.

[25] Cañizares, P.; García-Gómez, J.; Marcos, I.F.d.; Rodrigo, M.A.; Lobato, J. Measurement of mass-transfer coefficients by an electrochemical technique. *J. Chem. Educ.*, **2006**, *83*, 1204-1207.

[26] Aquino, J.M.; Rodrigo, M.A.; Rocha-Filho, R.C.; Sáez, C.; Cañizares, P. Influence of the supporting electrolyte on the electrolyses of dyes with conductive-diamond anodes. *Chem. Eng. J.*, **2012**, *184*, 221-227.

[27] Deborde, M.; Gunten, U.v. Reactions of chlorine with inorganic and organic compounds during water treatment—Kinetics and mechanisms: A critical review. *Water Res.*, **2008**, *42*, 13-51.

[28] Martínez-Huitle, C.A.; dos Santos, E.V.; de Araújo, D.M.; Panizza, M. Applicability of diamond electrode/anode to the electrochemical treatment of a real textile effluent. *J. Electroanal. Chem.*, **2012**, *674*, 103-107.

[29] Pereira, G.F.; Rocha-Filho, R.C.; Bocchi, N.; Biaggio, S.R. Electrochemical degradation of bisphenol A using a flow reactor with a boron-doped diamond anode. *Chem. Eng. J.*, **2012**, *198-199*, 282-288.

[30] Bensalah, N.; Alfaro, M.A.Q.; Martínez-Huitle, C.A. Electrochemical treatment of synthetic wastewaters containing Alphazurine A dye. *Chem. Eng. J.*, **2009**, *149*, 348-352.

FIGURE CAPTIONS

**Fig. 1**. Relative *COD* decay as a function of the applied electrical charge per unit volume of electrolyzed solution ($Q_{ap}$). All the experiments were carried out using 0.6 $dm^3$ of a 100 mg $dm^{-3}$ (0.25 mmol $dm^{-3}$) aqueous solution of AB 62 in 0.1 mol $dm^{-3}$ $Na_2SO_4$, pH 7, 35 ºC, at a flow rate of 400 $dm^3$ $h^{-1}$. Specific conditions: (◇) 30 mA $cm^{-2}$ and 0 mmol $dm^{-3}$ NaCl; (■) 10 mA $cm^{-2}$ and 20 mmol $dm^{-3}$ NaCl; (✳) 30 mA $cm^{-2}$ and 20 mmol $dm^{-3}$ NaCl; (△) 30 mA $cm^{-2}$ and 40 mmol $dm^{-3}$ NaCl; (◆) 50 mA $cm^{-2}$ and 20 mmol $dm^{-3}$ NaCl; (–··–) expected $COD_{rel}$ changes for 100% current efficiency. Lines refer to the values calculated using the model – see text: (–) 10 mA $cm^{-2}$, (---) 30 mA $cm^{-2}$, and (···) 50 mA $cm^{-2}$.

**Fig. 2**. Relative **(a)** *absorbance* (at 596 nm) and **(b)** *TOC* decay as a function of the applied electrical charge per unit volume of electrolyzed solution ($Q_{ap}$) for the experiments and specific conditions of Fig. 1. (–··–) expected $TOC_{rel}$ changes for 100% current efficiency. Lines refer to the values calculated using the model – see text: (–) 10 mA $cm^{-2}$, (---) 30 mA $cm^{-2}$, and (···) 50 mA $cm^{-2}$.

**Fig. 3**. First order kinetic constants as a function of **(a)** current density (for 20 mmol $dm^{-3}$ NaCl) and **(b)** NaCl concentration (at 30 mA $cm^{-2}$). Parameters: (◆) *Absorbance* at 596 nm, (□) *COD*, and (△) *TOC*; (×) refers to data for a purely mass transport-controlled kinetic constant. All the experiments were carried out using 0.6 $dm^3$ of a 100 mg $dm^{-3}$ (0.25 mmol $dm^{-3}$) aqueous solution of AB 62 in 0.1 mol $dm^{-3}$ $Na_2SO_4$, pH 7, 35 ºC, at a flow rate of 400 $dm^3$ $h^{-1}$.

**Fig. 4**. First order kinetic constants as a function of **(a)** temperature (at pH 7) and **(b)** pH (at 35 ºC), at 30 mA $cm^{-2}$, in the presence of 20 mmol $dm^{-3}$ NaCl. Parameters: (◆) *Absorbance* at 596 nm, (□) *COD*, (△) *TOC*; (×) refers to a purely mass transport-controlled kinetic constant. All the experiments were carried out using 0.6 $dm^3$ of a 100 mg $dm^{-3}$ (0.25 mmol $dm^{-3}$) aqueous solution of AB 62 in 0.1 mol $dm^{-3}$ $Na_2SO_4$, at a flow rate of 400 $dm^3$ $h^{-1}$.

**Fig. 5**. Instantaneous current efficiency (ICE) as a function of the **(a)** relative *COD* and **(b)** relative *TOC* decay. Conditions: (■) 10 mA $cm^{-2}$, 20 mmol $dm^{-3}$ NaCl, 35ºC, and pH 7; (✳) 30 mA $cm^{-2}$, 20 mmol $dm^{-3}$ NaCl, 35ºC, and pH 7; (◆) 50 mA $cm^{-2}$, 20 mmol $dm^{-3}$ NaCl, 35ºC, and pH 7; (◇) 30 mA $cm^{-2}$, 0 mmol $dm^{-3}$ NaCl, 35ºC, and pH 7; (△) 30 mA $cm^{-2}$, 40 mmol $dm^{-3}$ NaCl, 35ºC, and pH 7; (○) 30 mA $cm^{-2}$, 20 mmol $dm^{-3}$ NaCl, 15ºC, and pH 7; (+) 30 mA $cm^{-2}$, 20 mmol $dm^{-3}$ NaCl, 55ºC, and pH 7; (–) 30 mA $cm^{-2}$, 20 mmol $dm^{-3}$ NaCl, 35ºC, and pH 3, (×) 30 mA $cm^{-2}$, 20 mmol $dm^{-3}$ NaCl, 35ºC, and pH 11. All the experiments were carried out using 0.6 $dm^3$ of a 100 mg $dm^{-3}$ (0.25 mmol $dm^{-3}$) aqueous solution of AB 62 in 0.1 mol $dm^{-3}$ $Na_2SO_4$, at

a flow rate of 400 $dm^3$ $h^{-1}$. Lines refer to the values calculated from model: (–) 10 mA $cm^{-2}$, (---) 30 mA $cm^{-2}$, and (⋯) 50 mA $cm^{-2}$.

**Fig. 6**. **(a)** *COD* and **(b)** *TOC* removals as a function of the electrical energy consumption per unit volume of electrolyzed solution. Conditions: (■) 10 mA $cm^{-2}$, 20 mmol $dm^{-3}$ NaCl, 35ºC, and pH 7; (✳) 30 mA $cm^{-2}$, 20 mmol $dm^{-3}$ NaCl, 35ºC, and pH 7; (◆) 50 mA $cm^{-2}$, 20 mmol $dm^{-3}$ NaCl, 35ºC, and pH 7; (◇) 30 mA $cm^{-2}$, 0 mmol $dm^{-3}$ NaCl, 35ºC, and pH 7; (△) 30 mA $cm^{-2}$, 40 mmol $dm^{-3}$ NaCl, 35ºC, and pH 7; (○) 30 mA $cm^{-2}$, 20 mmol $dm^{-3}$ NaCl, 15ºC, and pH 7; (＋) 30 mA $cm^{-2}$, 20 mmol $dm^{-3}$ NaCl, 55ºC, and pH 7; (–) 30 mA $cm^{-2}$, 20 mmol $dm^{-3}$ NaCl, 35ºC, pH 3, (×) 30 mA $cm^{-2}$, 20 mmol $dm^{-3}$ NaCl, 35ºC, and pH 11. All the experiments were carried out using 0.6 $dm^3$ of a 100 mg $dm^{-3}$ (0.25 mmol $dm^{-3}$) aqueous solution of AB 62 in 0.1 mol $dm^{-3}$ $Na_2SO_4$, at a flow rate of 400 $dm^3$ $h^{-1}$.

**Fig. 1**

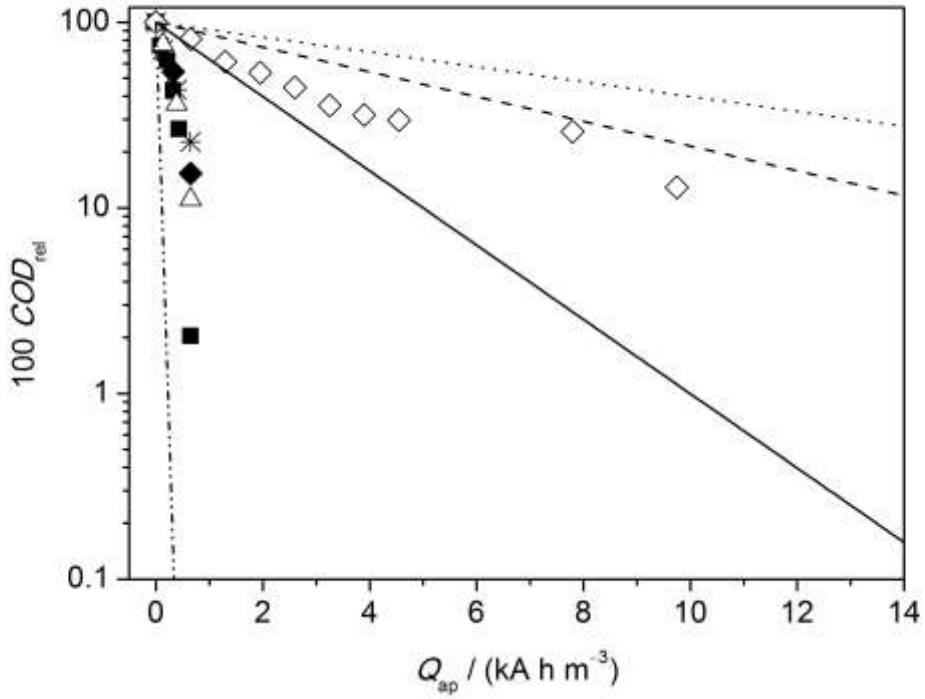

**Fig. 2a**

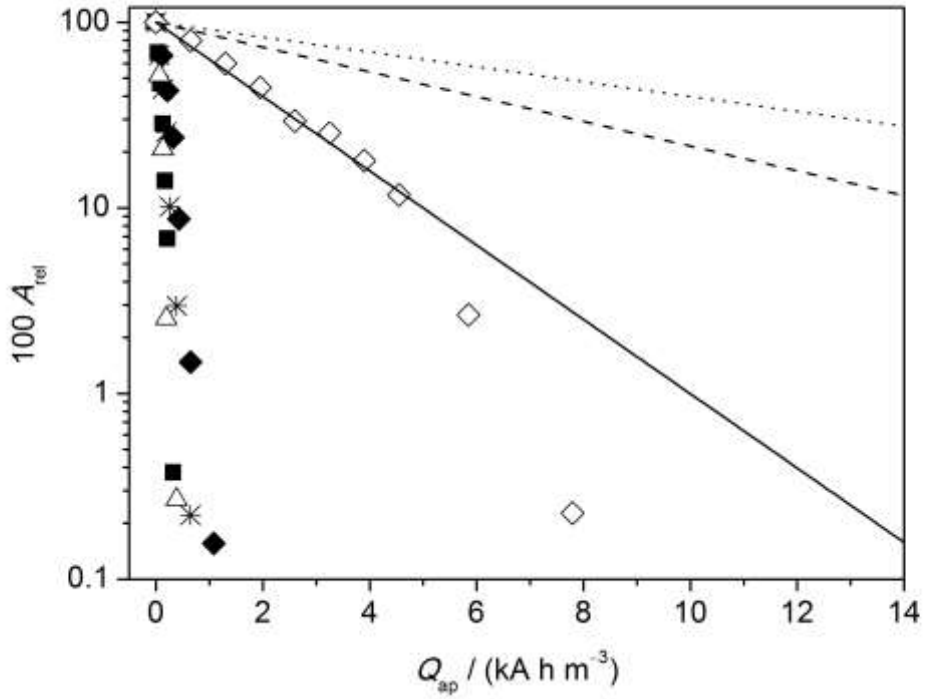

**Fig. 2b**

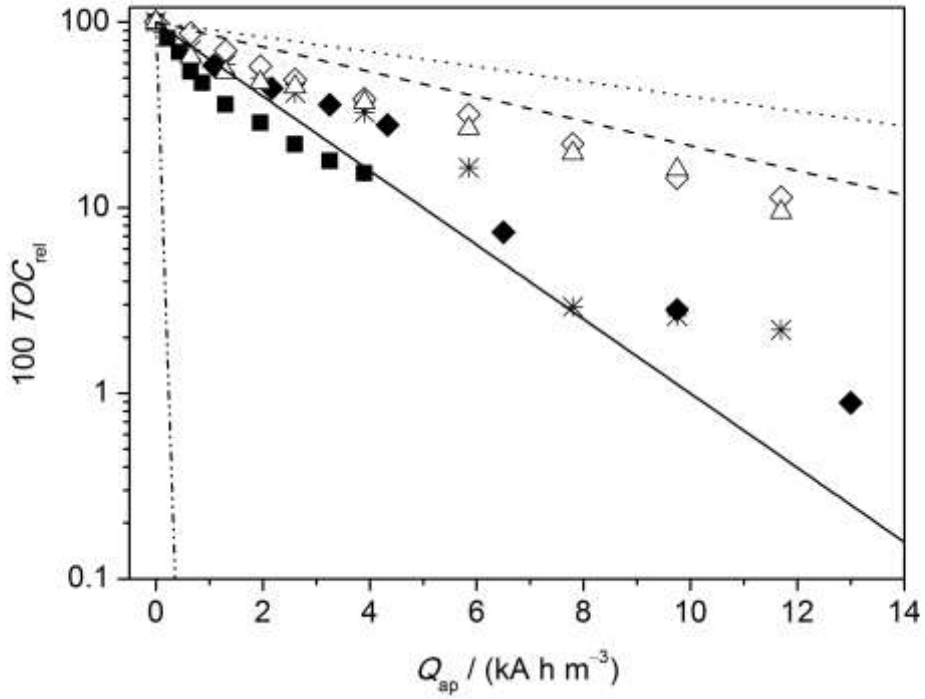

**Fig. 3a**

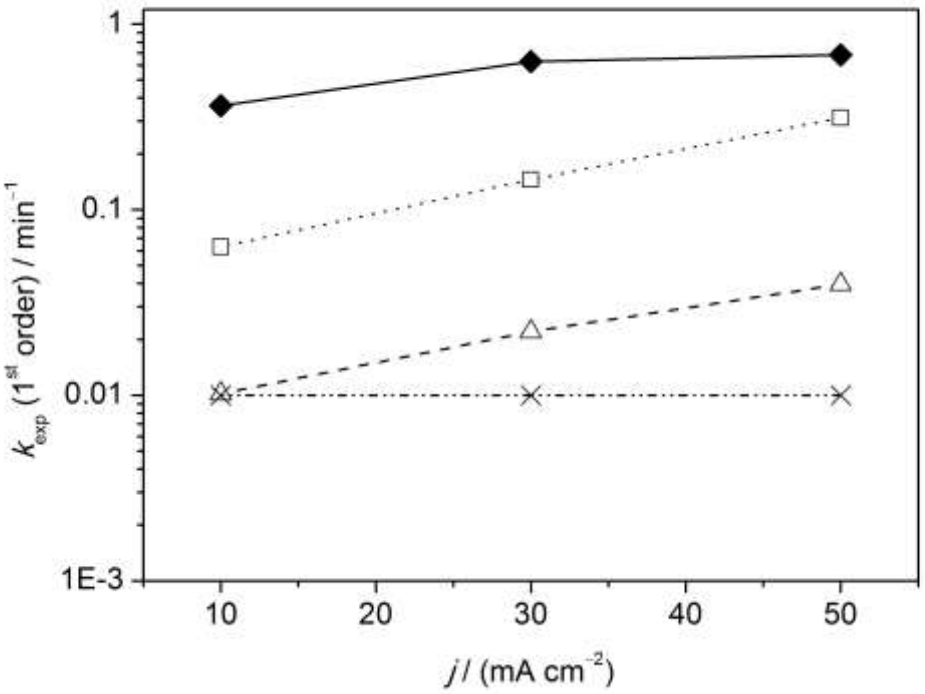

**Fig. 3b**

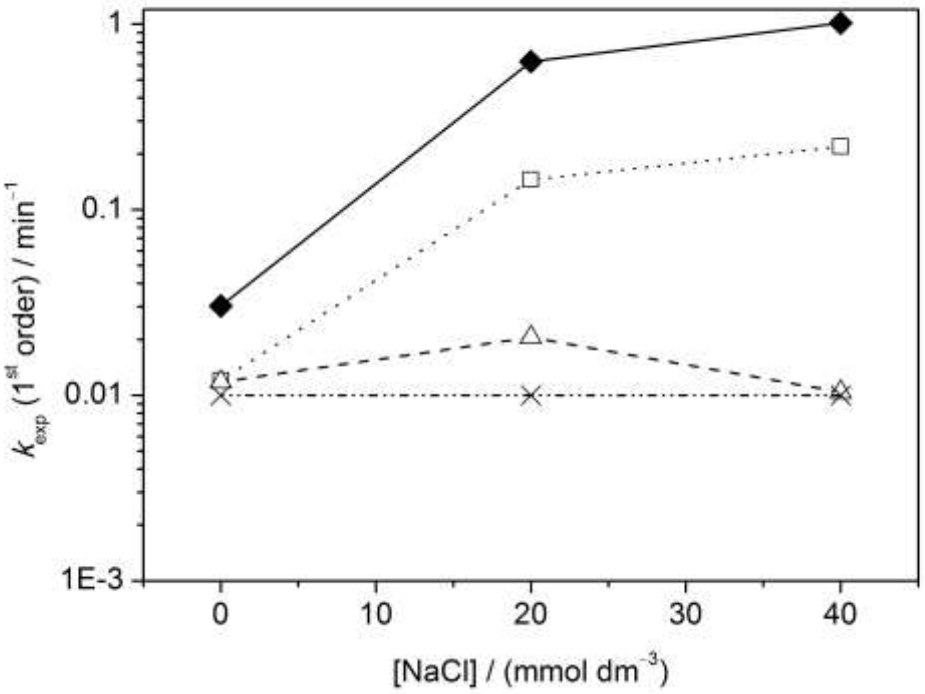

**Fig. 4a**

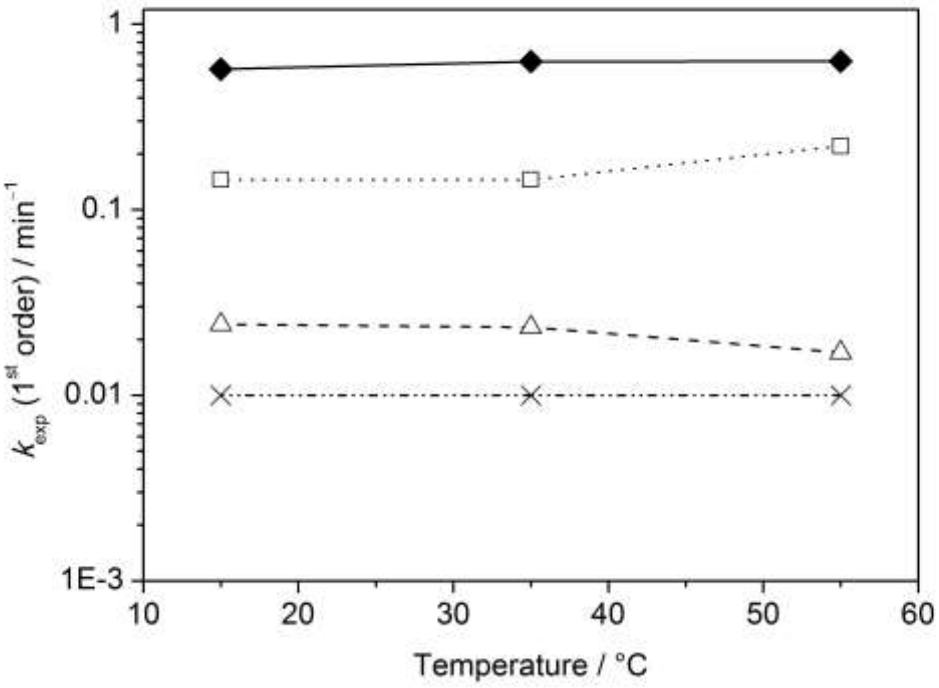

**Fig. 4b**

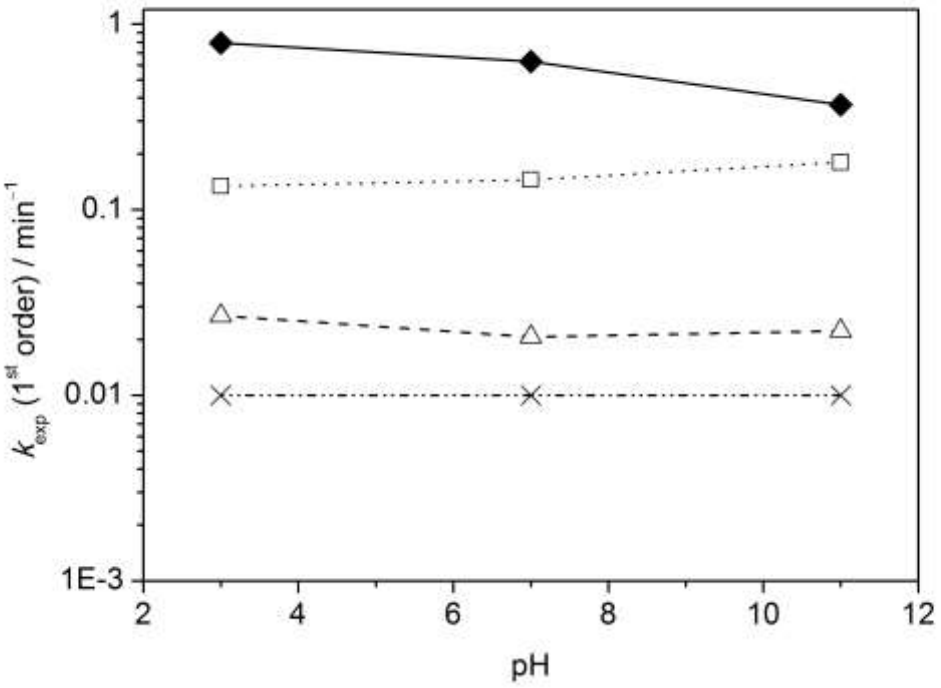

**Fig. 5a**

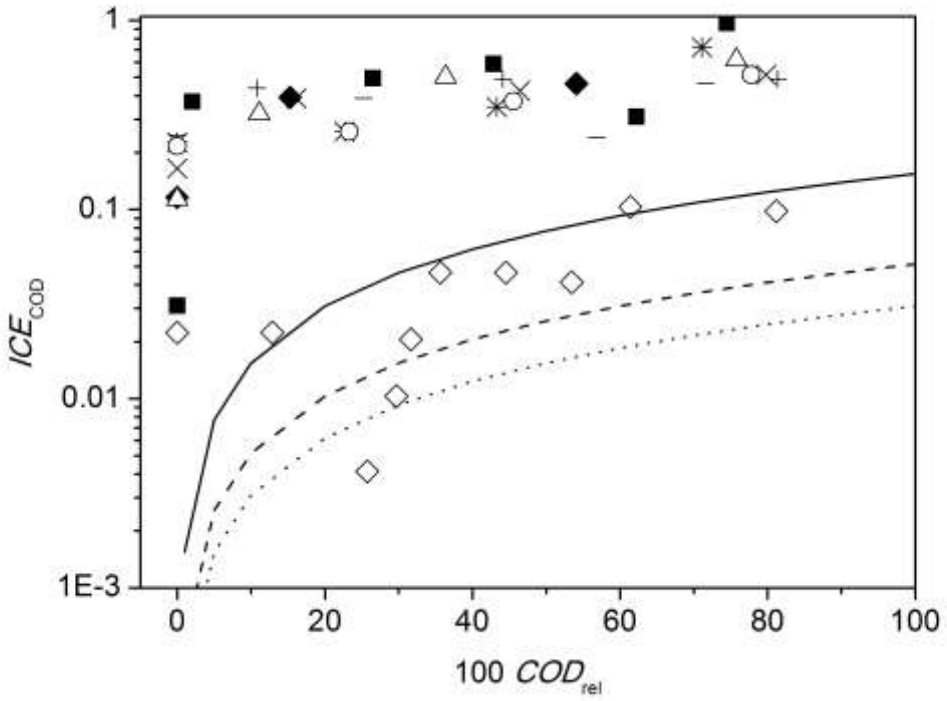

**Fig. 5b**

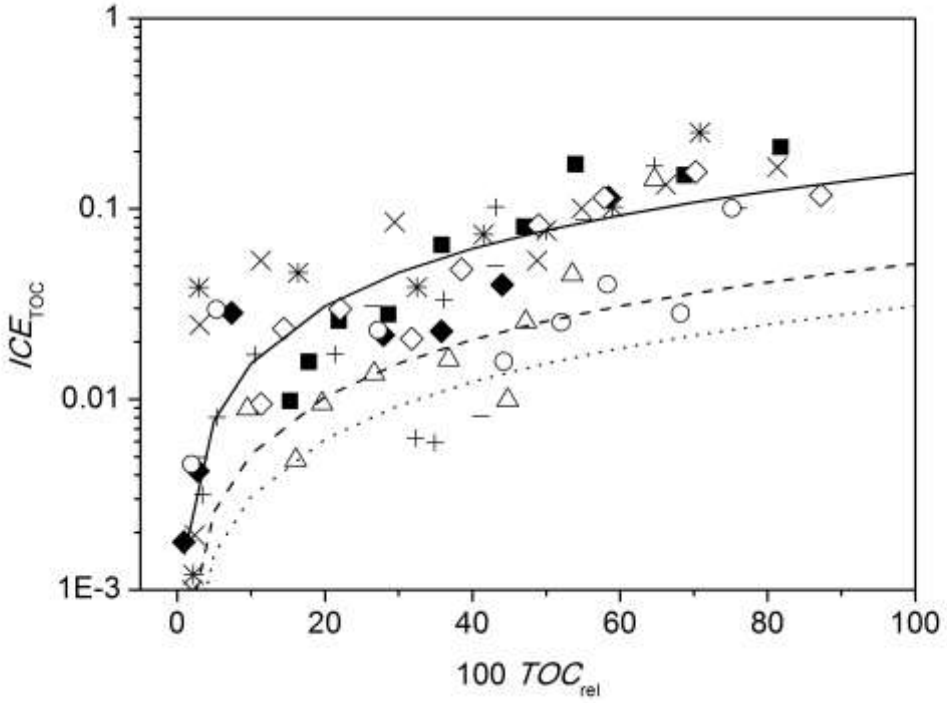

**Fig. 6a**

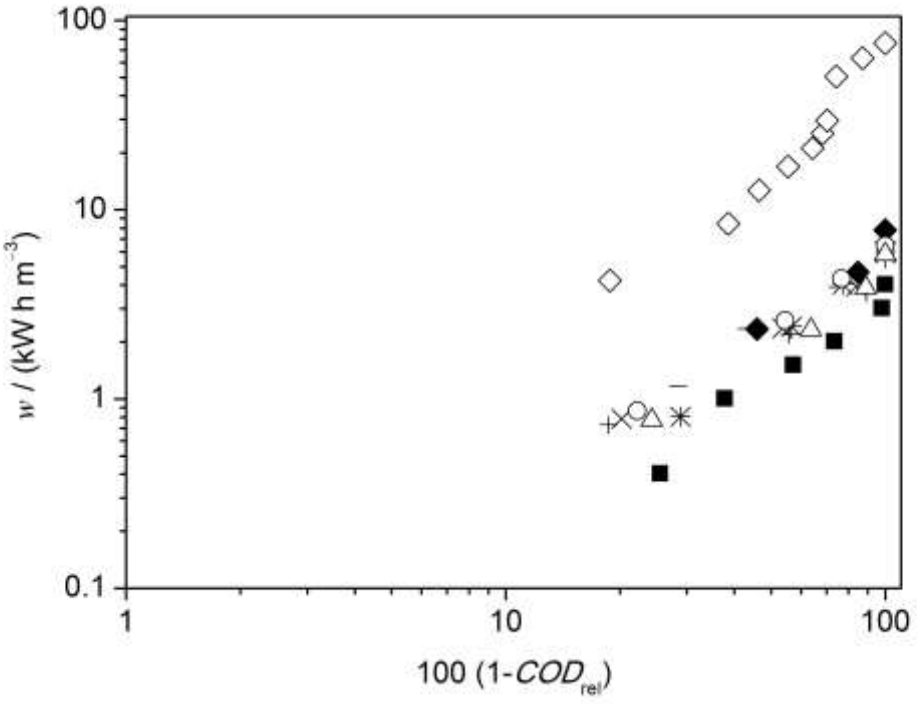

**Fig. 6b**